Preprints of the 19th World Congress
The International Federation of Automatic Control
Cape Town, South Africa. August 24-29, 2014

Fault-tolerant Control of a Master Generation Unit in an Islanded Microgrid

Luis Ismael Minchala-Avila * **Adriana Vargas-Martínez** *
Luis Eduardo Garza-Castañón * **Ruben Morales-Menendez** *
Youmin Zhang ** **Eduardo Robinson Calle-Ortiz** ***

* *Tecnológico de Monterrey, Campus Monterrey, Monterrey NL México, ismael.minchala@gmail.com, {adriana.vargas.mtz, legarza, rmm} @itesm.mx*
** *Concordia University, Montréal QC, Canadá, ymzhang@encs.concordia.ca*
*** *Universidad Politécnica Salesiana, Cuenca AZ, Ecuador, ecalle@ups.edu.ec*

Abstract: Two model-based fault-tolerant control design strategies are presented for a *Diesel Engine Generator (DEG)* working as a master generation unit in an islanded microgrid consisting of a hybrid wind-diesel-photovoltaic power system with a *Battery Storage System (BSS)*. A *Model Predictive Control (MPC)* scheme and a *Model Reference Adaptive Control (MRAC)* scheme have been selected for precise and stable voltage and frequency regulation in the *DEG*. A *Fault Detection and Diagnosis (FDD)* module is added to the *MPC* structure, in order to reconfigure the control strategy when actuator faults in the *DEG* are present. *MRAC* is used in combination with a *PID* controller tuned by a *Genetic Algorithm (GA)*. Improved performance over a baseline controller, *IEEE* type 1 *Automatic Voltage Regulator (AVR)*, is achieved in a developed realistic simulation environment based on Matlab/Simulink.

Keywords: Fault-Tolerant Control, Microgrids, Power systems

1. INTRODUCTION

The traditional way of delivering energy to the consumers has been experimenting changes from the topology point of view. Certainly, the most noticeable one is the installation of the smart meters. Additionally, another important concept related with improving energy delivery is the microgrid concept, for whose right integration into the main grid, some challenges need to be studied. One of those is the frequency and voltage regulation in interconnected electrical systems with multiple generation sources. Many different approaches have been studied and proposed for both grid-connected and islanded microgrid operation. Grid-connected operation relies on main grid parameters. On the other hand, islanded microgrid operation needs a frequency leader due to the high integration of *Renewable Energy Sources (RES)* whose intermittent characteristic due to climate dependability, complicates the use of traditional control schemes. For instance, a *Sliding Mode Control* for voltage amplitude regulation of a stand-alone synchronous generator connected to a resistive load is presented in Munoz-Aguilar et al. (2011), while in Kumar et al. (2008) a frequency regulator for a hybrid wind-diesel power system through multiple *PI* controllers is proposed. *LPV* control strategies have also been used for similar cases, where a *DEG* is feeding a group of loads He and Yang (2006) and interconnected with RES forming a hybrid power system, Croci et al. (2012). However, the above-mentioned works do not consider important issues on fault-tolerance of hybrid power systems for reliable electricity generation. This fact motivated the current research work to be presented in this paper.

This paper presents and extended discussion and performance comparison of two control approaches for controlling a master generation unit in a microgrid, one of them is deeply discussed as a *Fault-tolerant MPC* (*FTMPC*) presented in Minchala-Avila et al. (2013) and the other is a hybrid *FTC* detailed in this paper as the combination of an *MRAC* and a *PID* controller tuned by a *GA*.

This paper is organized as follows: Section 2 gives a brief description of the microgrid modeling. Section 3 deals with the controllers design. Section 4 presents simulation results and performance analysis and finally conclusions are drawn in Section 5. Acronyms are summarized at the end of the paper.

2. MODELING OF THE MICROGRID COMPONENTS

The microgrid that will be used as a study case for testing the proposed controllers is shown in Fig. 1, which is composed of different *Distributed Generation* (*DG*) units, such as: a *DEG*, a wind energy conversion system, a *PhotoVoltaic* (*PV*) array, two *BSS* and power converters. Since the main focus of this paper is to design the a fault-tolerant control strategy for the master generation unit, the *DEG* modeling procedure is to be presented: diesel engine and synchronous generator, while the modeling

⋆ This work was partially supported by *Tecnológico de Monterrey* through the *Supervision and Advanced Control* research chair.

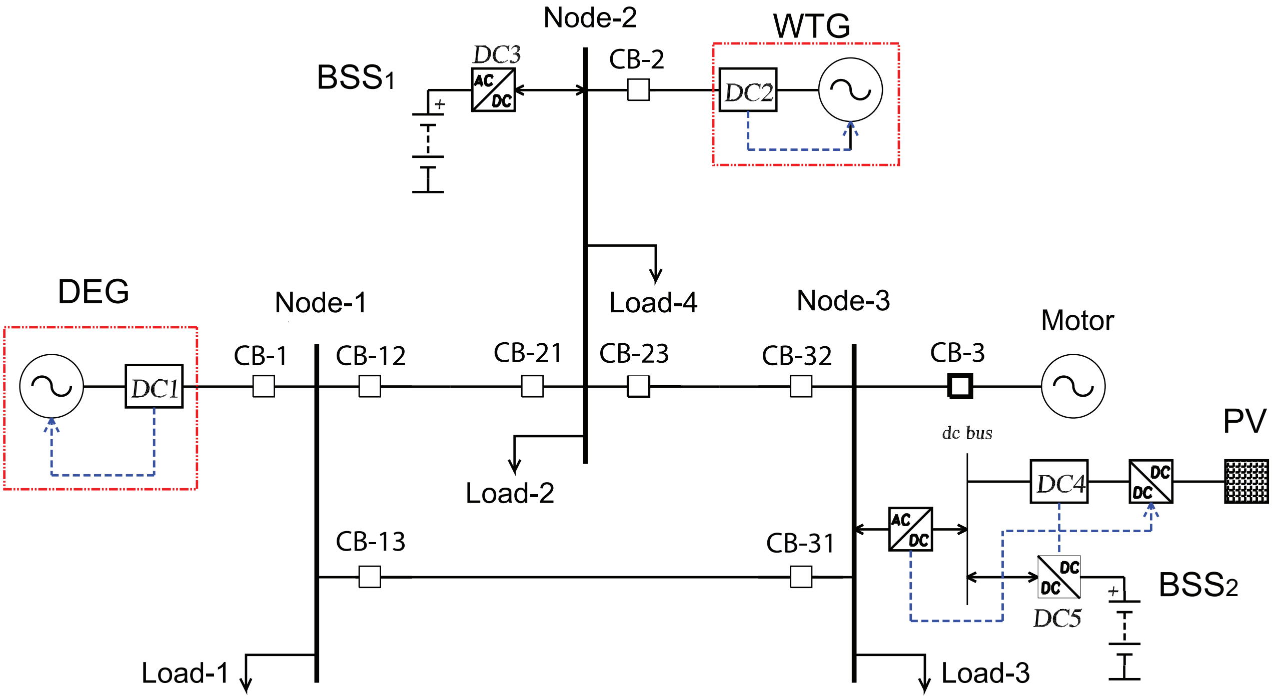

Fig. 1. Hybrid wind-diesel-photovoltaic power system architecture with *BSS*.

procedure of the other components are out of the scope of this paper.

2.1 Diesel engine generator

Diesel engine. Figure 2 shows a block diagram of the *Diesel Engine (DE)*. The actuator block is modeled by a first-order system with a gain K_a and a time constant T_a. On the other hand, the *DE* block contains the combustion system and it is responsible for the movement of the pistons and in consequence the crankshaft will generate a torque T_m in the shaft. Some research papers, Lee et al. (2008), use a time delay $e^{-\tau s}$ and a torque constant K_b for modeling this block. The flywheel block is an approximation of the inertia dynamics generated inside the machine, η represents the flywheel acceleration constant and the coefficient δ represents friction. State $x_1(t)$ represents the amount of fuel injected to the *DE*, which is one of the parameters to be minimized for an optimal integration of this *DG* unit into a microgrid.. The output $x_2(t)$ represents the angular velocity of the shaft of the engine. The input $d(t)$ is used for modeling load changes in the shaft of the rotor. The continuous-time model of the *DE* is represented in state-space equations, as follows:

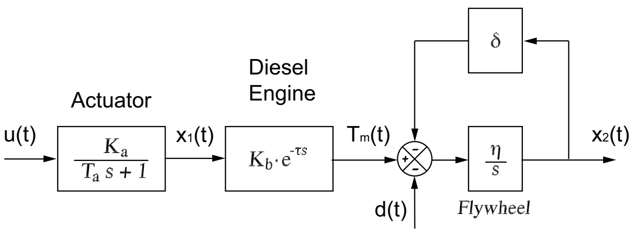

Fig. 2. Classic *DE* block diagram.

$$\dot{\mathbf{x}}(t) = \mathbf{A}_0\mathbf{x}(t) + \mathbf{A}_1\mathbf{x}(t-\tau) + \mathbf{B}_0 u(t) + \mathbf{F}d(t) \qquad (1)$$

$$\mathbf{A}_0 = \begin{bmatrix} -\frac{1}{Ta} & 0 \\ 0 & -\delta\eta \end{bmatrix} \quad \mathbf{A}_1 = \begin{bmatrix} 0 & 0 \\ \eta K_b & 0 \end{bmatrix}$$

$$\mathbf{B}_0 = \begin{bmatrix} \frac{K_a}{T_a} \\ 0 \end{bmatrix} \quad \mathbf{F} = \begin{bmatrix} 0 \\ -1 \end{bmatrix}$$

A state-space model using dynamic equations in the *dq* reference frame, through a Park's transformation for a pure resistive load R_L connected into the synchronous machine is presented in Munoz-Aguilar et al. (2011) and is summarized as follows:

$$\mathbf{L}\frac{d\mathbf{x}}{dt} = \mathbf{A}\mathbf{x} + \mathbf{B}v_F \qquad (2)$$

$$\mathbf{A} = \begin{bmatrix} -(R_s + R_L) & \omega L_s & 0 \\ -\omega L_s & -(R_s + R_L) & -\omega M_s \\ 0 & 0 & -R_F \end{bmatrix}$$

$$\mathbf{x} = \begin{bmatrix} i_d \\ i_q \\ i_F \end{bmatrix} \quad \mathbf{L} = \begin{bmatrix} L_s & 0 & M_s \\ 0 & L_s & 0 \\ M_s & 0 & L_F \end{bmatrix} \quad \mathbf{B} = \begin{bmatrix} 0 \\ 0 \\ 1 \end{bmatrix}$$

where $[\, i_d \; i_q \; i_F \,]^T$ are the *dq* stator and field currents, respectively; R_s and R_F are the stator and field resistances; L_s, L_m, and L_F are the stator, magnetizing, and field inductances; M_s represents mutual inductance; $\omega = 2\pi f$ is the electrical angular speed; v_d and v_q are the *dq* stator voltages; and v_F is the field voltage.

3. CONTROLLER DESIGN

Figure 1 depicts the hybrid power system architecture to be controlled, where *DC* stands for *Distributed Controller* and *CB* stands for *Circuit Breaker*. The microgrid was designed with Homer software. HOMER is a computer model that simplifies the task of designing *DG* systems - both on and off-grid, Homer Energy LLC (2013) .An

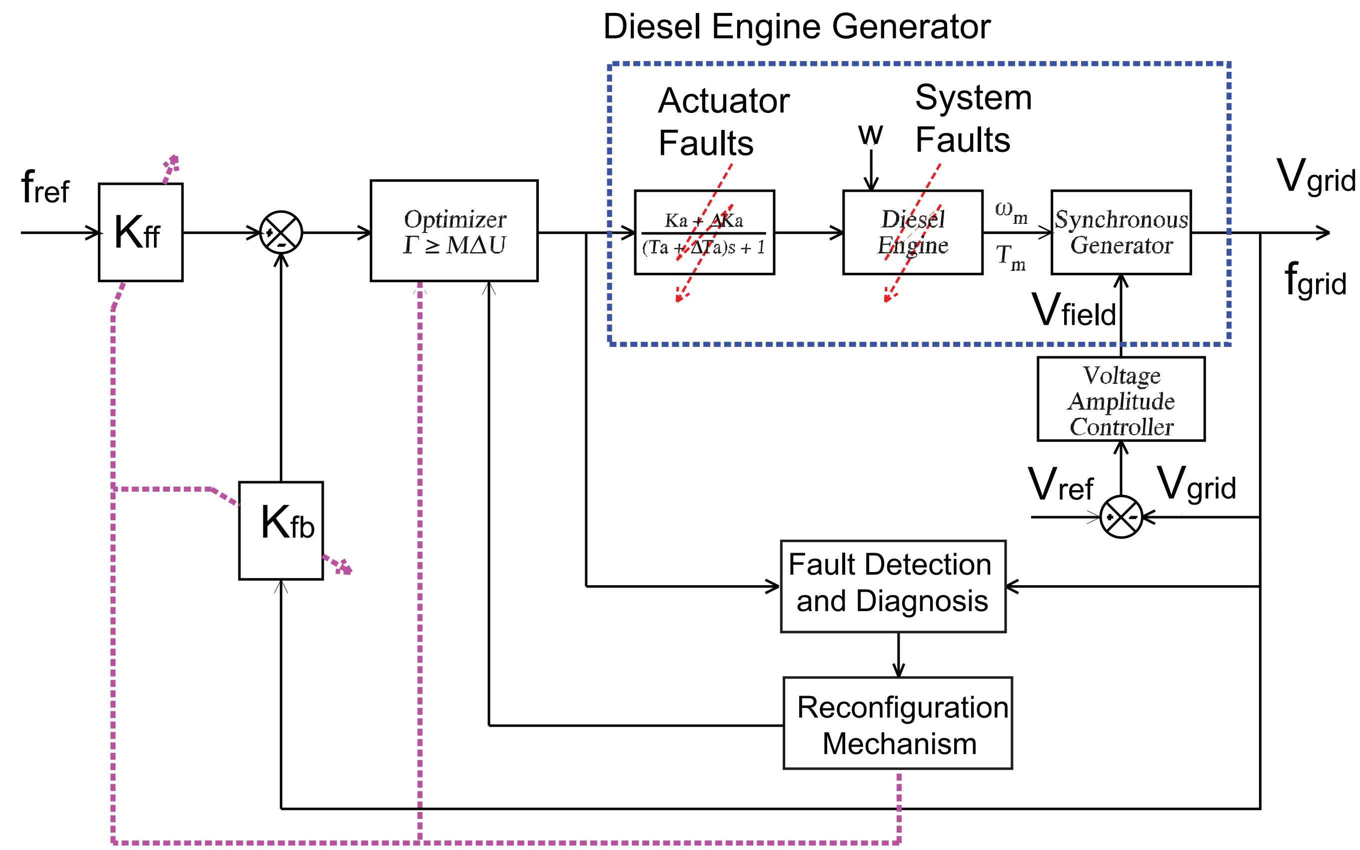

Fig. 3. Fault-tolerant *MPC* structure for the *DEG* control.

optimal microgrid architecture for *RES* integration is obtained with this software, although assumptions of perfect controllers for microgeneration units are considered in the optimization process and neither transient behavior nor stability issues of the microgrid are taken into account in this design. To overcome these drawbacks, the *DC* characteristics developed for this hybrid power system are:

(1) *DC1* implements two non-decoupled *MPC*s as a first approach and two *MRAC*s as a second approach, which are in charge of regulating grid frequency and voltage amplitude. A *DE* is used as a prime mover, which drags a synchronous generator at a constant speed. It is well known that the frequency of an islanded microgrid is determined by the mechanical speed ω_m which is provided by the *DE*, while the voltage amplitude is set by the synchronous generator field voltage.
(2) *DC2* is regarded to power generation control of the *Wind Turbine Generator (WTG)*, which works in the power rated zone. An *MPC* for a limited range of the blade pitch angle, $0 < \beta < 15$, is implemented. The *WTG* is tested in power-rated region of operation under a variable wind speed profile.
(3) *DC3* controls a bi-directional AC-to-DC converter to manage battery charge and discharge. A three-phase, full-wave and phase-controlled rectifier is used for AC-to-DC conversion, while for DC-to-AC conversion a bridge type *IGBT Voltage Source Inverter (VSI)* controlled through *Space Vector Pulse Width Modulation (SVPWM)* Abu-Rub et al. (2012), has been implemented.
(4) *DC4* represents an *MPPT* circuit implemented in a DC-to-DC boost converter for power extraction from the *PV* array. Switching duty cycle for the boost converter is optimized by the *MPPT* controller with the incremental conductance technique, Kish et al. (2012) and the addition of an integral regulator.
(5) *DC5* represents a bi-directional DC-to-DC converter and also is in charge of controlling power conversion of the DC-to-AC converter which links the DC bus with node 3. Therefore, the *PV* array is connected to the utility grid by a boost converter *(DC4)* and a *VSI*. Meanwhile, the battery is connected to the common DC bus via a bi-directional DC-to-DC converter. A buck-boost converter is used, whose purpose is to charge the battery when there is enough generating power and to support load perturbations and lower power generation from the *PV* array due to climate changes, *e.g.* sun occlusions.

3.1 MPC Design

MPC is an optimal control algorithm capable of managing constraints in its structure. An accurate model of the system is needed in order to predict the response of the system over a prediction horizon, N_p, to an optimal predicted control input $\hat{u}(k+i|k)$, where $k < i < k+N_c$, N_c represents the control horizon and $\hat{u}(k+N_c-1|k) = \hat{u}(k+N_c-1+i|k)$ for $N_c < i < N_p$. Most *MPC* designs are formulated in discrete-time with a fixed sampling period. A discrete-time state-space representation for the system to be controlled is:

$$\mathbf{x}(k+1) = f(\mathbf{x}(k), \mathbf{u}(k)), \qquad k \in \{0, 1, 2, ...\} \tag{3}$$

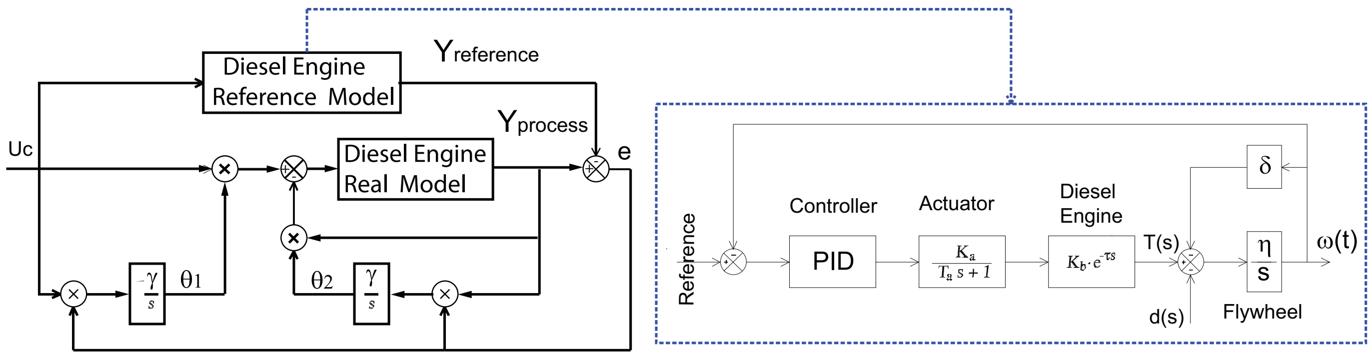

Fig. 4. *MRAC-PID* control structure for regulating speed of *DE*.

where $\mathbf{x}(k)$ represents the state vector and $\mathbf{u}(k)$ is the system input. Since *MPC* allows constraints management, both $\mathbf{x}(k)$ and $\mathbf{u}(k)$ are to be restricted according to:

$$\mathbf{x}(k) \in \mathbb{X} \in \mathbb{R}^n \qquad \mathbf{u}(k) \in \mathbb{U} \in \mathbb{R}^p \tag{4}$$

A cost function has to be selected for the controller design. The following choice encompasses many alternatives documented in the literature, Cortes et al. (2008):

$$J(\mathbf{x}(k), \mathbf{u}(k)) = F(\mathbf{x}(k + N_p)) + \sum_{i=k}^{k+N_c-1} L(\mathbf{x}(i), \mathbf{u}(i)) \tag{5}$$

where $F(\cdot)$ and $L(\cdot)$ are weighting functions for penalizing predicted system behavior. *MPC* is achieved by performing a constrained optimization of (5) for finding an optimal control sequence, $\mathbf{u}(k) = \{\hat{u}(k), \hat{u}(k+1), \ldots, \hat{u}(k+N_c-1)\}$. The optimization yields an optimal control sequence where only the first element is used for controlling the system, while the whole optimization procedure is repeated in each sampling step.

To provide fault-tolerance to the classic *MPC*, an *FDD* module is added to its structure, and proper decisions regarding the information from this module have to be taken. Therefore, a *Fault-Tolerant MPC (FTMPC)* is composed of the *MPC*, *FDD* module and a reconfiguration mechanism as the general structure of *FTC* system outlined in Zhang and Jiang (2008), as shown in Fig. 3.

A combination of the parity space technique and a *Kalman Filter (KF)* is proposed for the *FDD* module design. Since the reconfiguration mechanism relies on the *FDD* module, it is important to guarantee an accurate fault detection and diagnosis. The *KF* recursively estimates the *DE*'s actuator model, while the parity space residual generator is able to detect an actuator fault with high reliability, avoiding false alarms and unnecessary control system reconfiguration if only the *KF* would be used.

Using the post-failure model estimated by the KF, the reconfiguration mechanism recalculates the controller gains K_{ff} and K_{fb}, and the constraint matrices $\mathbf{M}$ and $\mathbf{\Gamma}$ shown in Fig. 3, Minchala-Avila et al. (2013).

3.2 MRAC Design

An *MRAC* performs a closed-loop controller that embraces the parameters that must be optimized in order to change the system response to accomplish the desired or ideal output. The adaptation mechanism modifies the controller parameters to match the real output with the reference model output. The reference model represents the ideal model behavior. Even though there are different schemes to design an *MRAC* controller, the *MRAC* used in this paper is based in *Lyapunovs* methodology in view of its advantage for guaranteeing system stability. This methodology demands finding a *Lyapunov*'s function, $V \in \mathbb{R}^n$, positive definite whose time derivative must be negative definite or semidefinite. In Vargas-Martínez et al. (2013), the proposed *Lyapunov* function is given as follows:

$$V(e, \theta_1, \theta_2) = \frac{1}{2}\left(a_{1r}e^2 + \frac{b_r}{\gamma}(\theta_1 - 1)^2 + \frac{b_r}{\gamma}(\theta_2)^2\right) \tag{6}$$

where b_r, γ and $a_{1r} > 0$. Equation (6) will be zero when the error is zero and the controller parameters are equal to the desired values.

The *MRAC* is combined with a classic *PID* controller tuned by a *GA* in order to overcome the limitations of the classic *MRAC* structure, *i.e.* limited fault accommodation threshold in comparison with the one of the *MRAC* combined with other structures. The *PID* controller is placed in the feedforward loop of the classic *MRAC*, as it is shown in Fig. 4 where the control structure of the *MRAC-PID* for regulating *DE*'s speed (frequency of the grid) is presented. The *PID* controller parameters were obtained by using a *GA* search to track the desired system trajectory with the help of Matlab - Optimization Toolbox. In this scheme, the desired closed-loop behavior of the system is established using the model reference trajectory, *i.e.* no faults in the system.

On the other hand, the voltage regulation is done by manipulating field voltage of the synchronous generator through a classic *MRAC*. This control scheme is shown in Fig. 5 *MRAC* provides the advantage of accommodating any deviation of the system, either these deviations are faults or perturbations.

4. SIMULATION RESULTS

The system architecture shown in Fig. 1 was implemented in Matlab/Simulink®. Four different controllers were tested in the *DEG (DC1)*, without changing the controllers structure in *DC2, DC3, DC4* and *DC5*. The first scheme implemented is the baseline control system for speed and voltage control that Matlab has in its library, *i.e.* governor and *PI* controller for the rotor speed control and the *IEEE* type 1 *AVR* for maintaining the

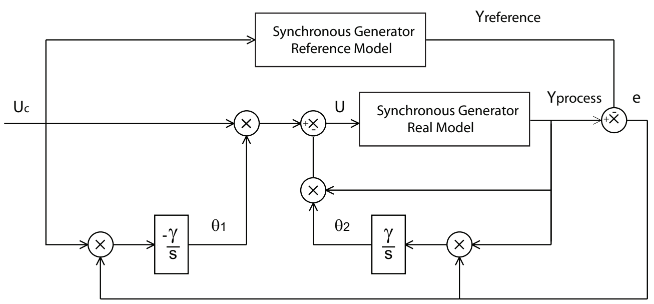

Fig. 5. *MRAC* scheme for voltage regulation.

voltage amplitude of the microgrid. Afterwards, an *MPC* without fault-tolerance was implemented. The third controller was the *FTMPC*. Finally, *MRAC-PID* is tested. Variable profiles for wind velocity (m/s) and solar irradiance $\left(W/m^2\right)$ were used during the simulation. Different operating conditions were tested in order to evaluate and compare robustness of the controllers. These events are shown in Table 1.

Table 1. Events in the simulation

Event	Time of occurrence (s)
Diesel only generation	$0 < t < 12$
WTG ignition	$t = 15$
BSS-1 charging process	$25 < t < 60$
BSS-2 charging process	$25 < t < 60$
Actuator degradation induced of 50%	$t >= 40$
$L_3 = \frac{1}{2}$ MW connection	$t >= 50$
PV array connection	$t >= 80$
3-Ph fault at Node 3	$t = 100$
CB-31 clears fault	$t = 100.5$
Stabilization period	$100.5 < t < 110$
Steady-state behavior	$110 < t < 130$

Figure 6 compares the comparison of the performance of the system for the *DEG*'s output variables. Both frequency and voltage amplitude are shown for the four control strategies. It is noticeable from Fig. 7 the fact that the baseline control system and the *MPC* without fault-tolerance conduct the system to instability after the actuator fault occurs, while the *FTMPC* and the *MRAC* are able to maintain system stability and to achieve satisfactory performance in maintaining desired synchronous generator output voltage and *DE* rotor speed for all the operating events presented in the simulation. Apart from the important control objectives of voltage and frequency regulation in the microgrid, supply energy for the balanced load is also a very important task that must be satisfied in a microgrid operation,

$$P_{DEG} = P_{total\ load} - P_{WTG} - P_{PV} \pm P_{BSS} \qquad (7)$$

where $\pm$ represents the possibility of a charging and discharging process of the *BSS*. Figure 7 shows the power generated by the *DEG, WTG, PV* and *BSS*. It is noticeable the fact that a correct power balance has been achieved; consequently a stable and reliable islanded microgrid operation can be guaranteed.

In this paper a concrete *BSS* strategy for optimal charge and discharge of the batteries was not considered and it will be part of the near future work. Additionally, since distributed controllers are spread in the microgrid a two-layer control strategy is next step of the research for integrating optimal dispatch of energy and load coverage once the microgrid is operating in islanding mode.

5. CONCLUSIONS

Two fault-tolerant controllers have been tested for controlling a *DE* working as a master generation unit in an islanded microgrid configuration. Compared with a baseline control system, the developed control strategies: *FTMPC* and *MRAC-PID* achieved significantly better performance when regulating voltage and frequency of the microgrid, while guaranteeing energy supply for the demand load. The scenario of simulation included steady state, transient and fault events in order to test robustness of the controllers . The controller reconfiguration used in the *FTMPC* leads to a simple approach that does not involve any switching operation, which could lead to instability problems. Since *MPC* recalculates its output at every sampling time, the reconfiguration operation would be another loop calculation per se. On the other hand, *MRAC* has an inherent capability to accommodate perturbations, faults and model uncertainties. However, the use of only this type of controller has a limited fault accommodation threshold. To overcome this issue, an *MRAC* was combined with a *PID* controller in order to guarantee systems stability under actuator faults in the *DEG*.

REFERENCES

Abu-Rub, H., Iqbal, A., and Guzinski, J. (2012). *High Performance Control of AC Drives with Matlab/Simulink Models*. Wiley.

Cortes, P., Kazmierkowski, M., Kennel, R., Quevedo, D., and Rodriguez, J. (2008). Predictive Control in Power Electronics and Drives. *IEEE Trans on Ind Electronics*, 55(12), 4312–4324.

Croci, L., Martinez, A., Coirault, P., and Champenois, G. (2012). Control Strategy for Photovoltaic-Wind Hybrid System using Sliding Mode Control and Linear Parameter Varying Feedback. In *IEEE Int Conf on Ind Technology*, 205–210.

He, B. and Yang, M. (2006). Robust LPV Control of Diesel Auxiliary Power Unit for Series Hybrid Electric Vehicles. *IEEE Trans on Power Electronics*, 21(3), 791–798.

Homer Energy LLC (2013). www.homerenergy.com.

Kish, G., Lee, J., and Lehn, P. (2012). Modelling and Control of Photovoltaic Panels utilising the Incremental Conductance Method for Maximum Power Point Tracking. *IET Renewable Power Generation*, 6(4), 259–266.

Kumar, B., Mishra, S., Bhende, C., and Chauhan, M. (2008). PI Controller based Frequency Regulator for Distributed Generation. In *TENCON - IEEE Conf*, 1–6.

Lee, S., Yim, J., Lee, J., and Sul, S. (2008). Design of Speed Control Loop of A Variable Speed Diesel Engine Generator by Electric Governor. In *IAS - IEEE Ind Applications Society Annual Meeting*, 1–5.

Minchala-Avila, L., Vargas-Martínez, A., Zhang, Y., and Garza-Castañón, L. (2013). A Model Predictive Control Approach for Integrating a Master Generation Unit in a Microgrid. In *Conf on Control and Fault-Tolerant Systems*, 674–679.

Munoz-Aguilar, R., Doria-Cerezo, A., Fossas, E., and Cardoner, R. (2011). Sliding Mode Control of a Stand-

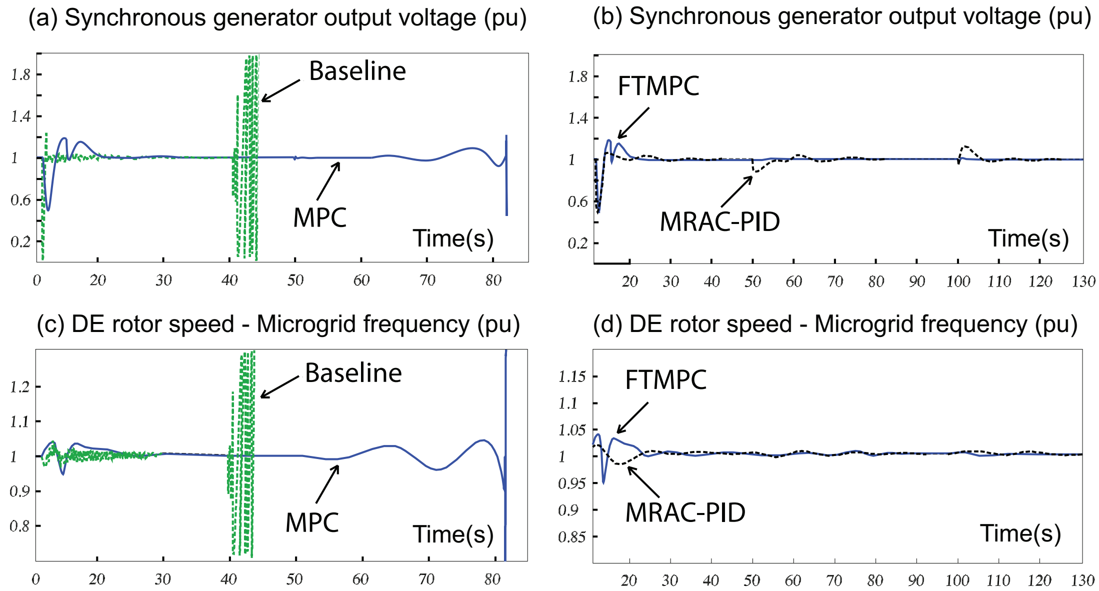

Fig. 6. Comparison of the control systems performance for the *DEG*.

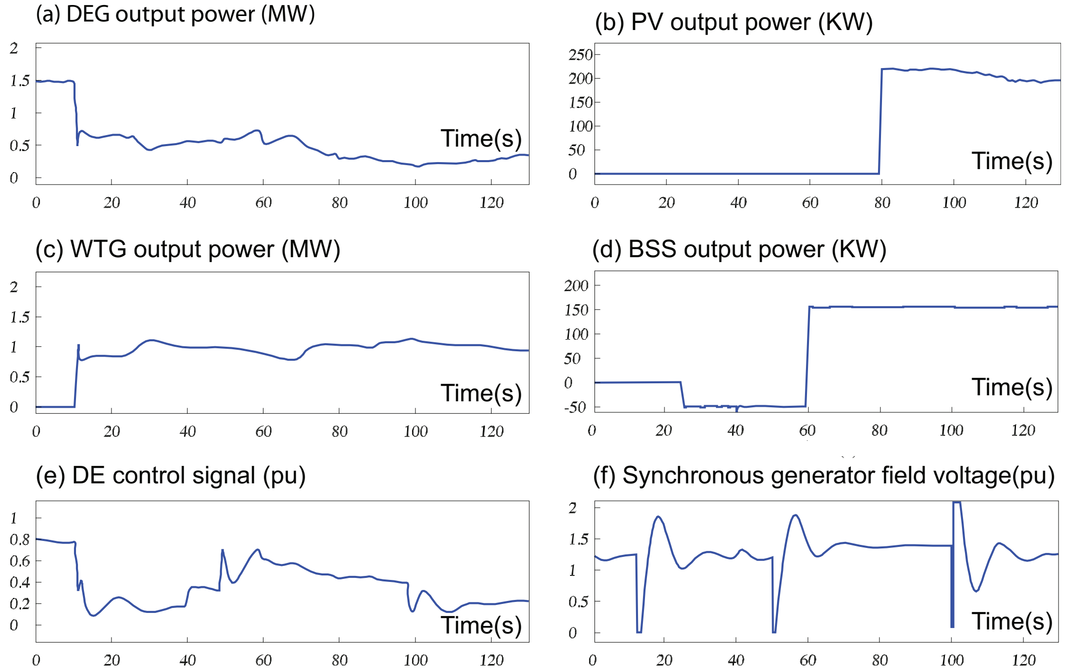

Fig. 7. Power generated by *DEG, WTG, PV* and *BSS*.

Alone Wound Rotor Synchronous Generator. *IEEE Trans on Ind Electronics*, 58(10), 4888–4897.

Vargas-Martínez, A., Garza-Castañón, L., Puig, V., and Morales-Menendez, R. (2013). Fault Tolerant Control for a Second Order LPV System using Adaptive Control Methods. In *IFAC Joint Conf* 5^{th} *Symp on System Structure and Control*, 852–857.

Zhang, Y. and Jiang, J. (2008). Bibliographical Review on Reconfigurable Fault-Tolerant Control Systems. *Annual Reviews in Control*, 32(2), 229–252.

	Acronyms
AFTC	Active Fault-tolerant Control
AVR	Automatic Voltage Regulator
BSS	Battery Storage System
DE	Diesel Engine
DG	Distributed Generation
DEG	Diesel Engine Generator
FDD	Fault Detection and Diagnosis
GA	Genetic Algorithm
MPC	Model Predictive Control
MRAC	Model Reference Adaptive Control
PV	PhotoVoltaic
PID	Proportional-Integral-Derivative
RES	Renewable Energy Source
WT	Wind Turbine
WTG	Wind Turbine Generator